Chiang Mai J. Sci. 2013; 40(4) : 763-774
http://epg.science.cmu.ac.th/ejournal/
Contributed Paper

Using Alumina and Zirconia Ceramic Composite in Dogs: A Biocompatibility Study

Korakot Nganvongpanit*[a,b], Alongkot Phothawan [b,c], Waranee Pradit [b,d], Sukum Eitssayeam [b,c], Jongkolnee Settakorn [e], Siriwadee Chomdej [b,d] and Supamit Mekchay [f]

[a] Bone and Joint Research Laboratory, Department of Veterinary Biosciences and Public Health, Faculty of Veterinary Medicine, Chiang Mai University, Chiang Mai 50100, Thailand.
[b] Materials Science Research Center, Faculty of Science, Chiang Mai University, Chiang Mai 50200, Thailand.
[c] Department of Physics and Materials Science, Faculty of Science, Chiang Mai University, Chiang Mai 50200, Thailand.
[d] Department of Biology, Faculty of Science, Chiang Mai University, Chiang Mai 50200, Thailand.
[e] Department of Pathology, Faculty of Medicine, Chiang Mai University, Chiang Mai, Thailand.
[f] Department of Animal Science, Faculty of Agriculture, Chiang Mai University, Chiang Mai 50200, Thailand.
*Author for correspondence; e-mail: korakot.n@cmu.ac.th

Received: 5 March 2012
Accepted: 21 December 2012

ABSTRACT

This research was to study the biocompatibility of in-house ceramic materials; consisted of different ratios of magnesium-doped alumina (MDA) and yttria-stabilized zirconia (YSZ). Materials 1-3 (M1-3) were 40, 50 and 60% MDA, respectively. Six male dogs were used for subcutaneous implants in the right hind limb for a 12-week period. Blood was collected from dogs weekly to evaluate health. Tissue surrounding material was then collected for histological evaluation and real-time PCR. Five transcripts, including TNF-α, IL-6, IL-13, IFN-g and MMP-9, were quantified using real-time PCR. The hardness of all materials was tested prior to and after implantation. The results found that all of the biopsy specimens showed neither foreign body reaction nor granulation tissue formation. Compared to the control, expression of MMP-9 in M1 was found to be significantly down-regulated ($P < 0.05$); expression of TNF-α, IL-13 and MMP-9 in M2 was found to be significantly different ($P < 0.05$); and in M3, IL-13 was found to be significantly up-regulated ($P < 0.05$). Hardness in M1 was significantly decreased ($P < 0.05$) after 12 weeks of implantation. In conclusion, M3, which consisted of 60% MDA, is a candidate material for use as a bone substitute in dogs.

Keywords: biocompatibility, ceramic, magnesium-doped alumina, yttria-stabilized zirconia, gene expression, dog

1. INTRODUCTION

In the last 20 years, applications for ceramics in orthopedics have continuously increased throughout the world. Nowadays, the development of artificial bone ceramic material has become a promising approach for repair of bone defects or for use as a

prosthesis. The first ceramic material has been in clinical use since 1971; currently up to 5 million components have been implanted [1-3]. Presently, numerous materials are available as all-ceramic core materials, such as leucite-reinforced ceramics, glass-infiltrated ceramics, lithium disilicate, alumina and zirconia [4]. Scientists recently have developed a new ceramic composite for clinical application in both medicine and veterinary medicine. This ceramic composite is a reinforced alumina, in which zirconia particles are stabilized in tetragonal phase, which is the phase that presents the best mechanical performance [5].

Each material has certain advantages for use in the synthesis of a ceramic composite. One of these materials alone is not a suitable choice for a medical ceramic. However, it is necessary to ascertain the optimal proportion of each material in order to achieve the best mechanical and biocompatibility properties. In this study, three combinations of an alumina and zirconia composite were selected as candidate materials for bone and joint implants. Until today, investigations carried out for these materials have been based on their mechanical and biocompatibility properties.

Surgical-grade alumina is obtained by sintering alumina powder at temperatures between 1,600 and 1,800°C. The resultant material is in its highest state of oxidation, allowing thermodynamic stability, chemical inertness, and excellent resistance to corrosion.

Alumina is a brittle material with excellent compression strength, but its bending strength is limited. The Young's modulus is 300 times greater than that of cancellous bone, and 190 times higher than polymethyl methacrylate (PMMA). Alumina has been a standardized material since 1984 (International Standard Organization, ISO 6474) [6].

Zirconia is a polymorphic crystal that can be found in three crystallographic forms: monoclinic (M), cubic (C) and tetragonal (T). Zirconia is monoclinic at room temperature, being stable up to 1,170°C. Above this temperature it becomes tetragonal, and over 2,370°C it passes to the cubic phase; this is stable until the melting point at 2,380°C is reached [7]. The properties of dense alumina and zirconia of surgical grade are summarized in Table 1.

A great deal of research had been conducted on the mechanical and biocompatibility properties of alumina and zirconia ceramics. Some factors - such as the proportions of alumina and zirconia, the sintering temperature, and others - affect the molecular structure and tissue reaction. This research aimed to study the biocompatibility property of an alumina and zirconia ceramics which was synthesized by our laboratory. This material was used to generate canine bone and joint substitutes. This study observes the effect of those materials using histopathology change and gene expression profile.

Table 1. Comparative physical properties of alumina and zirconia ceramics of surgical grade [6].

Property	Alumina	Zirconia
Purity (%)	>99.8	97.0
Density (g/cm^3)	3.98	6.05
Grain size (μm)	3.6	0.2 to 0.4
Surface finish (Ra, μm)	0.02	0.008
Bending strength (MPa)	595	1,000
Compressive strength (MPa)	4,250	2,000
Young's modulus (GPa)	380	210
Hardness (Vickers hardness number)	2,000	1,200
Fracture toughness KIC (MN/m$^{3/2}$)	5	7

2. MATERIALS AND METHODS

2.1 Preparation of Ceramic Material

Three blends of the materials used in this study were tested for performance and mechanical properties by the Materials Science Research Center, Faculty of Science, Chiang Mai University [8]. These consisted of different ratios of magnesium-doped alumina (MDA) and yttria-stabilized zirconia (YSZ). Materials 1-3 (M1-3) were 40, 50 and 60% MDA, respectively.

Animals

This experiment was performed using 6 healthy adult male dogs, each weighing between 15-20 kg. All animal were determined to be healthy by clinical examination and blood checks. Animals were kept in separate cages (0.8×1.0× 1.0 m). The room temperature was controlled between 25-30°C. The animals were subcutaneously implanted with materials 1, 2 and 3 (M1, M2, M3) in the right lateral hind limb. Each material was 5 cm in length. All implantations were performed with the animal under anesthesia using 5 mg/kg tiletamine+zolazepam (Zoletil®; Virbac Laboratories, Carros, France) in sterile conditions. A prophylactic antibiotic (20 mg/kg cefazolin; Nida Pharma, Bangkok, Thailand) and an anti-inflammatory drug (4.4 mg/kg carprofen; Rimadyl®; Pfizer, Thailand) were given intravenously in three doses over a 24 h period during and after surgery. The experimental protocol was approved by the Faculty of Veterinary Medicine and the Ethics Committee, Chiang Mai University, Thailand.

Blood collection and biochemical analysis

Throughout the experiment, blood was collected 14 times (once a week), 2 times before implantation and 12 times after. Five ml blood samples were collected from the cephalic vein of each dog. All blood samples were taken prior to the morning feeding. One ml of blood sample from each dog was kept in anticoagulant (100 IU/ml heparin) for a complete blood count (CBC). Two ml of blood sample was centrifuged to obtain the serum at 10,000 × *g* for 15 min and kept frozen at -20°C until blood chemistry was performed.

Biochemical analyses, CBC and blood chemistry were conducted at the Small Animal Hospital, Faculty of Veterinary Medicine, Chiang Mai University, Chiang Mai, Thailand. Blood samples were analyzed for CBC including hematocrit (HCT), hemoglobin (Hb), red blood cell count (RBC), white blood cell count (WBC) and platelet count. Two ml of serum was used to analyze blood chemicals, including

aspartate aminotransferase (AST), alanine aminotranferase (ALT), blood urea nitrogen (BUN) and creatinine.

Material implantation

The materials were implanted laterally in the right hind limb (Figure 1). Tissue was harvested 12 weeks (3 months) after implantation. The tissues were divided into two parts. The first part was fixed in 10% formalin (Sigma, Thailand) for histology; the second part was kept at -80°C for RNA extraction. Moreover, all ceramic materials were used for hardness testing to compare before and after embedding.

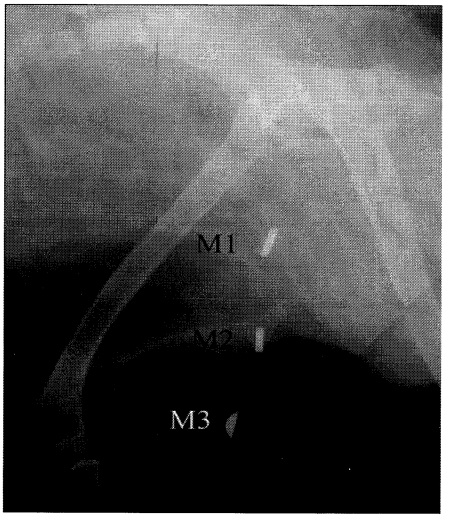

Figure 1. Radiographs of implanted materials (lateral view).

Histology evaluation

For histology evaluation, skin was collected at the implant site and fixed with 10% buffered formalin. All tissue samples were embedded in paraffin, sectioned and stained with hematoxylin and eosin (H&E) for evaluation by light microscopy. Tissue biopsies were evaluated by two pathologists blinded to material type.

RNA isolation

Total RNA was extracted using the InviTrap® Spin Universal RNA Mini Kit (Invitek, Berlin, Germany) following the manufacturer's instructions. Briefly, samples homogenized in liquid nitrogen were lysed in 600 ml of DTT containing Lysis Solution TR. The lysate was centrifuged for 2 min at 13,000× *g*; then the supernatant was transferred to a new tube for genomic DNA removal with 330 ml of 96-100% ethanol. Next, the lysate was transferred to an RTA Spin Filter set, incubated for 1 min at room temperature, and centrifuged for 1 min at 10,000× *g*. After that, 600 ml of Wash Buffer R1 were added onto the RTA Spin Filter, centrifuged at 10,000× *g* for 30 s, and the flow-through discarded. The washing step with 600 ml of Wash Buffer R2 was performed by centrifuging at 10,000× *g* for 30s. An additional protocol for DNA digestion on the RTA Spin Filter was performed by adding 10 ml of a DNase reaction mixture directly in the center of the filter membrane; this was incubated for 10 min at room temperature. Six hundred ml of Wash Buffer R2 was added onto the filter, incubated for 1 min, and centrifuged for 30 s at 10,000 × *g*. The addition of 600 ml of Wash Buffer R2 was carried out again without the incubation step. To eliminate any traces of ethanol, centrifugation for 5 min was performed at 13,500× *g*. Thirty ml of Elution Buffer R were added directly onto the membrane of the RTA Spin Filter, incubated for 2 min at room temperature, centrifuged for 1 min at 10,000× *g* to collect the total RNA, and then stored at -80°C.

cDNA synthesis

Total RNA was converted to first-strand cDNA using RevertAid™ Reverse Transcriptase (Fermentas; Burlington, Ontario, Canada) with oligo$(dT)_{18}$ (Bio Basic; Markham, Ontario, Canada). Reverse transcription was performed by first

annealing 10 nmol of oligo$(dT)_{18}$ to 10 mg of total RNA by incubation at 65°C for 5 min, and then placing on ice until the addition of the remaining component to achieve a final concentration of 1X buffer, 1 mM dNTPs, 40 U RiboLock™ RNase Inhibitor (Fermentas, Canada) and 200 U RevertAid Reverse Transcriptase. The mixture was incubated at 37°C for 5 min, at 42 C for 90 min, and then inactivated at 70°C for 10 min.

Quantitative real-time PCR

Five transcripts - tumor necrosis factor-alpha (TNF-α), interleukin-6 (IL-6), interleukin-13 (IL-13), interferon-gamma (IFN-γ) and matrix metalloproteinase 9 (MMP-9) - were quantified in all groups of skin using glyceraldehyde-3-phosphate dehydrogenase (GAPDH) as an endogenous control [9-12]. One ml of reversely transcribed total RNA was amplified with Maxima® SYBR Green qPCR Master Mix (2X) and ROX Solution (Fermentas), in a volume of 25 ml with specific amplification primer pairs (Table 2). PCR amplification was operated using a Chromo4™ System (Bio-Rad, Hercules CA, USA) with the following protocol: 95°C for 15 min, 45 cycles of denaturation for 15 s at 94°C, annealing for 30 s at different annealing temperatures, and extension at 72°C for 30 s with a final extension at 72°C for 10 min. Fluorescent data were acquired after each extension step. A melting curve was generated after 45 cycles by slowly heating the sample from 65 C at 0.2°C, while the fluorescence was measured at intervals until the temperature increased to 95°C. Finally, the results were analyzed and reported as relative expression value after normalization to the endogenous control.

Table 2. Set of primers used for real-time quantitative PCR.

Gene	Primer sequence (5'→3')	Length(bp)	Accession no.
GAPDH	Fw: AGTATGATTCTACCCACGGC	362	DQ403060
	Rw: CGAAGTGGTCATGGATGACT		
TNF-α	Fw: AGTGCCGTCAGATGGGTTG	215	NM_001003244
	Rw: CCAGGTAGATGGGCTCGTA		
IL-6	Fw: TGGCTACTGCTTTCCCTAC	189	NM_001003301
	Rw: GTGCCTCTTTGCTGTCTTC		
IL-13	Fw: CGCTCTGGTTGACTGTGGT	130	NM_001003384
	Rw: GATGCCTGATTCTGGGTGA		
MMP-9	Fw: TTTCGCTATGGCTACACTCAA	377	NM_001003219
	Rw: TGCTCCCTAACACCAAACTGA		
IFN-γ	Fw: AGGTCCAGCGCAAGGCGATA	117	NM_001003174
	Rw: TCGATGCTCTGCGGCCTCGAA		

bp = base pair

Hardness test

Vickers hardness tests were used in this study to test before and after implantation [8]. Briefly, the technique involved testing the hardness of materials using a High Quality Hardness Tester (Buehler, Lake Bluff, IL, USA). The pressure force applied to the material was 200 gf (gram-force) for 15 s, at five locations on each material.

Statistical analysis

The mRNA expression analysis for studied genes in all treatment groups was based on the relative standard curve method. All data were analyzed using the Statistical Analysis System (SAS) version 8.0 (SAS Institute, Cary NC, USA) software package. Differences in mean values between two or more experimental groups were tested using ANOVA, followed by multiple pairwise comparisons using a *t*-test. Differences of $P < 0.05$ were considered to be significant.

3. RESULTS

3.1 CBC and Blood Chemistry

Table 3 shows the value ranges for each parameter in all animals. All values were not significantly different throughout the experimental period ($P < 0.05$). Moreover, no animals showed signs of infection or illness throughout the experimental period.

Table 3. Complete blood count and blood chemistry during the experimental period.

weeks	0	1	2	3	4	5	6	7	8	9	10	11	12
Hematocrit (%)	41-46	39-52	40-46	40-44	39-44	39-44	39-45	39-45	41-46	41-45	41-43	41-44	41-45
Hemoglobin (g/dl)	9.0-11.0	9.0-11.4	9.4-11.5	9.2-10.9	9.8-11.0	9.5-10.9	9.9-11.2	9.6-11.0	9.7-10.9	9.3-11.0	9.3-11.2	9.4-11.0	9.8-10.9
WBC count (cell/µl)	11,242-16,538	12,523-18,535	11,242-18,635	12,525-20,012	9,421-19,843	10,021-19,732	10,753-18,473	7,422-13,424	10,531-19,424	9,453-17,436	9,213-17,435	14,324-19,843	10,753-16,426
Neutrophil (%)	63-83	68-80	63-83	67-84	68-84	54-86	64-87	57-81	59-86	52-84	34-86	59-81	59-79
Lymphocyte (%)	12-24	14-29	15-25	14-27	13-31	13-29	14-29	13-24	15-27	13-26	14-27	13-27	14-26
Monocyte (%)	3-11	4-16	2-13	4-14	3-9	2-12	6-11	2-19	4-17	3-18	1-16	2-11	4-11
Eosinophil (%)	2-5	1-5	2-5	2-4	2-4	2-4	2-5	1-5	1-5	1-3	1-6	2-5	1-5
Basophil (%)	0-1	0-1	0-2	0-1	0-1	0-2	0-1	0-2	0-2	0-1	0-1	0-1	0-1
AST (U/L)	52-96	89-113	78-116	82-143	85-123	53-102	64-97	52-112	59-99	46-105	64-115	93-105	87-143
ALT (U/L)	45-77	50-96	45-97	58-98	44-102	46-113	61-96	59-101	45-80	61-97	66-95	58-89	46-102
BUN (mg/dl)	14-33	12-43	15-30	13-36	8-32	15-37	15-27	12-25	11-36	14-34	12-32	13-37	14-26
Creatinine (mg/dl)	0.1-1.0	0.1-1.1	0.20.5	0.2-1.1	0.5-1.1	0.2-1.1	0.2-10.2	0.3-1.1	0.3-1.0	0.4-1.2	0.1-1.1	0.2-0.9	0.2-0.6

All blood results are in normal range.

3.2 Histological Change

All of the biopsy specimens showed neither foreign body reaction nor granulation tissue formation (Figure 2). There was only a mild degree of superficial chronic perivascular inflammation, with few lymphocytes and histiocytes in the skin of M1 and M3 groups. The tissues from the M2 group revealed a moderate degree of chronic perivascular and periadnexal inflammation, with a few lymphocytes and histiocytes. Scar formation was observed in 1 out of 2 in the M1 group, 2 out of 3 in the M2 group, and 1 out of 3 in the M3 group. Neutrophils were not found in any group.

3.3 Related Gene Expression

The results of mRNA quantification showed four genes - TNF-α, IL-13, MMP-9 and IFN-γ-that had a significant difference between groups, while the expression of IL-6 was not significantly different ($P > 0.05$) between groups (Figure 3). The TNF-α expression in the M2 group was significantly lower ($P < 0.05$) than in the control and other groups. The expression of IL-13 in the M2 group was significantly lower ($P < 0.05$) than in the control group, while it was found to be significantly higher ($P < 0.05$) in the M3 group than in the control group. For MMP-9 expression, M1 and M2 groups were

significantly lower ($P < 0.05$) than the control group, but the M3 group showed no difference ($P > 0.05$). There was no significant difference ($P > 0.05$) between experiment groups and the control group, but expression on the targeted gene was significantly lower ($P < 0.05$) in the M2 group than in the other two groups (M1 and M3).

3.4 Hardness Test

Material 1 showed a significant decrease in hardness ($P < 0.05$) after 3 months implantation. The other two materials also showed a decrease in hardness after implantation, but not a significant difference (Figure 4).

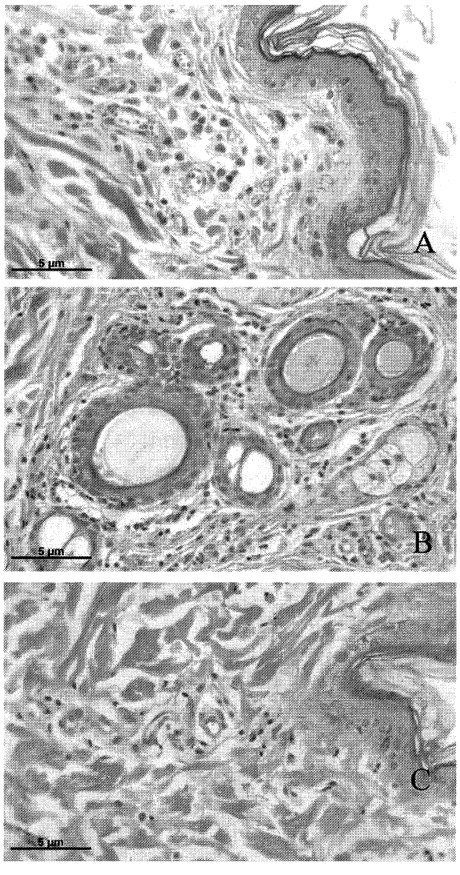

Figure 2. Representative photomicrographs of the dog skin around materials 1 (A), 2 (B) and 3 (C).

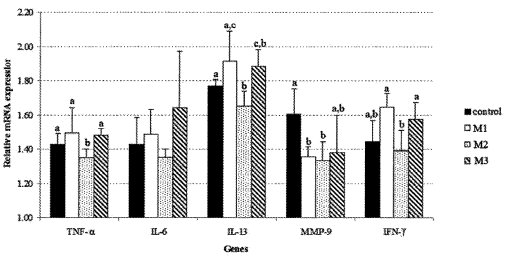

Figure 3. Relative expression of tumor necrosis factor-alpha (TNF-α), interleukin-6 (IL-6), interleukin-13 (IL-13), matrix metalloproteinase 9 (MMP-9) and interferon-gamma (IFN-g) in all experimental groups. Individual bars show the mean ± SD. Significant differences ($P<0.05$) between the four groups are indicated by superscripts (a,b,c) on the bars.

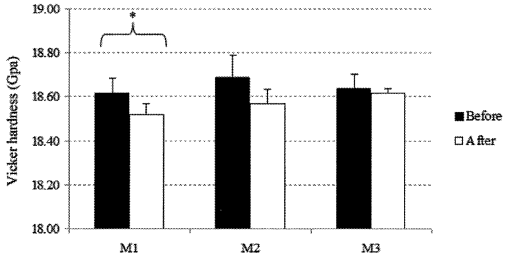

Figure 4. Vickers hardness test of all materials before and after embedding in dogs. A significant difference ($P < 0.05$) was found between before and after embedding with the same material.

4. DISCUSSION

The foreign body reaction, composed of macrophages and foreign-body giant cells, is the end-stage response of the inflammatory and wound-healing responses following implantation of a medical device, prosthesis or biomaterial. In the present study we showed that, in the implantation of ceramic material in the skin of dogs, different ratios of MDA and YSZ did not induce inflammation, but induced correlated gene expression.

The number of animals used in this study was limited due to animal ethics concerns.

However, we used an internal control, and animals in both groups showed the same result. Our model has the advantage of prolonged exposure of material. This study was designed to observe a long implantation period, 3 months, for which no data had previously been published. We did not collect tissue samples for histological evaluation and gene expression study during the early phase of this study (such as 1 week or 1 month after implantation) because some prior studies had shown no effects during the early post-implantation period [13]. However, we did not observe any clinical signs of inflammation at the implantation site from the day of implantation; this, together with blood results, did not reveal any signs of infection or illness.

Bacterial contamination of the material is an important factor; bacterial contamination is a possible consequence of surgery. Bacterial adhesion, which is important in the problem-free maintenance of zirconia restorations, has been proven to be satisfactorily low [14-15]. Scarano and colleagues reported the degree of bacterial coating to be 12.1% in zirconia, compared to 19.3% in titanium [15]. Another confirmation of these results was from an *in vivo* study in which crystals of zirconia accumulated fewer bacteria than titanium, in terms of total number of bacteria [14].

Tissue reactions following implantation of any biomaterial can include acute inflammation, chronic inflammation, pain, granulation tissue development, and fibrous capsule formation [16]. Previous studies [13-16] involving biocompatibility tests have usually used histology and immunohistochemistry to evaluate the effects of a material on tissue. This study is the first to use real-time PCR to quantify the gene expression of tissue around the implanted material. This study selected some important genes which respond to the inflammation process, including TNF-α, IL-6, IL-13, IFN-γ and MMP-9.

Tumor necrosis factor is a cytokine produced primarily by macrophages in response to stimuli activating toll-like receptors, but can also be expressed by activated T cells, B cells and NK cells [17]. It is synthesized as a 26 kDa membrane-bound protein. The TNF- ectodomain is cleaved at the cell surface to a soluble 17 kDa protein by a metalloproteinase-like enzyme that has been designated TNF-α-converting enzyme (TACE). The 17 kDa protein is considered the mature product, but there are data to suggest that the 26 kDa membrane-associated protein could be implicated in direct cell: cell interactions. The tumor necrosis factor-converting enzyme is also known as ADAM17, as it is part of the larger ADAM family (ADAM: proteins containing a disintegrin and metalloproteinase domain), and is inhibited by tissue inhibitor of metalloproteinase-3 (TIMP-3) [18]. TNF-α is a multipotent cytokine which plays a part in apoptosis, cell activation, cell recruitment and differentiation [17]. This study found that TNF-α in M2 was significantly lower than in the other groups; while TNF-α in M1, M3 and the control showed no significant difference.

IL-6 belongs to a family of gp130 receptor ligands that includes IL-11, leukemia inhibitory factor, ciliary neurotrophic factor, oncostatin M, and cardiotrophin-1 [19]. IL-6 has long been regarded as a proinflammatory cytokine induced by lipopolysaccharides, along with TNF-α and IL-1. IL-6 is often used as a marker for systemic activation of proinflammatory cytokines [20]. IL-6 down-regulates the synthesis of IL-1 and TNF [21], while it induces the synthesis of glucocorticoids [22]. Our study did not find the expression of IL-6 transcript significantly different

between groups. Due to an early response to the inflammation process of IL-6, it is possible that the time for study of IL-6 expression in our study was delayed for 3 months after implanting the material.

IL-6 and TNF-α are proinflammatory cytokines which play an important role in immune response and activation of the inflammatory process [23]. These cytokines are induced by IFN-γ. Previous studies have shown that increasing TNF-α can induce apoptosis [24]. IFN-g is the prototypical T helper (Th) cell cytokine, but it is also produced by natural killer (NK) cells. The central biological actions described for IFN-γ are macrophage activation, antiviral activity, antiproliferative activity on tumor cells, production of free radicals, and induction of expression of adhesion molecules, as well as those of MHC class I and II [25]. In this study, the expressions of IFN-g in all materials were not significantly different compared with the control group. However, a comparison of the three materials found that the IFN-γ gene was expressed significantly lower in M2 than in the other two materials.

IL-13 is produced by natural killer and NKT lymphocytes in a degranulation process, and plays a significant role in determining the extent and degree of subsequent development of the foreign body reaction [26]. It is a 132-amino-acid nonglycosylated protein with a molecular weight of about 10 kDa [27]. IL-13 and IL-4 are the only cytokines with the ability to promote IgE switch recombination [28]. IL-13 can down-regulate the production of TNF, IL-1, IL-8 and MIP-1α by monocytes, and has profound effects on expression of surface molecules in both monocytes and macrophages [29]. Previous studies have shown that IL-13 up-regulates cell surface expression of β_2 integrins and major histocompatibility complex (MHC) class II antigens, and down-regulates CD14 and Fcγ receptor expression. IL-13 inhibits NF-κB activation in macrophages and protects against LPS-induced lethality in animal models [20, 30]. This study found expression of IL-13 in M2 significantly down-regulated compared to the control, while expression in M1 and M3 were up-regulated; but this was significantly higher only in M3. It is possible that the up- and down-regulation of the IL-13 transcript was due to the response of lymphocytes to the materials.

One disadvantage of this research is that we did not study the expression of IL-13-related transcription, such as IL-1, IL-4 and IL-8 due to the volume of mRNA was not enough to study. However, a comparison of the ratios between IL-13 and TNF-α in the control, M1, M2 and M3 groups -1.24±0.06, 1.28±0.03, 1.23±0.05 and 1.27±0.06, respectively - found no significant difference between groups.

In order to further understand how macrophages can influence extracellular matrix (ECM) remodeling and wound healing, the secretion of MMPs was studied. Matrix metalloproteinases are proteolytic proteins that hydrolyze components of the extracellular matrix [31]. MMP-9 or gelatinase B are believed to be the critical enzymes for degrading type IV collagen, a major component of the basement membrane. It is thought that the secretion of gelatinases having specificity for type IV collagen can endow endothelial cells with an advantage for degradation of the extracellular matrix and subsequent migration across the basement membrane [32]. In this study, expression of MMP-9 was found to have a significantly lower response to M1 and M2 compared to the control and M3. It possible that M1 and M2 do not induce the remodeling process of tissues around those materials.

Moreover, our study focused on the

results of the hardness test after 3 months' implantation. The hardness of all materials prior to this showed no difference. After 3 months, the hardness was significantly decreased in M1,while others were unchanged. It is believed that changes in the hardness of M1 after implantation are due to a reaction from the animal immune system. This means that M1 is not a good candidate for use as a biomaterial. However, in deep explants this reaction cannot explain the mechanics of this reaction, which requires further study. In a comparison of M2 and M3, histological findings showed no difference between the two materials; but most of the expression of mRNA in M3 was not significant compared to the control.

Taking all of these results into account, we recommend future study of certain aspects of M3, such as long-term (more than one year) *in vivo* testing, before use of this material as a bone substitute.

ACKNOWLEDGEMENTS

The authors would like to acknowledge financial support via research grants from the National Research University Project under Thailand's Office of the Higher Education Commission.

REFERENCES

[1] Nizard R.S., Sedel L., Christel P., Meunier A., Soudry M. and Witvoet J., Ten-year survivorship of cemented ceramic-ceramic total hip prosthesis, *Clin. Orthop. Relat. Res.*, 1992; 53-63.

[2] Hamadouche M., Boutin P., Daussange J., Bolander M.E. and Sedel L., Alumina-on-alumina total hip arthroplasty: A minimum 18.5-year follow-up study, *J. Bone Joint Surg. Am.*, 2002; **84-A:** 69-77.

[3] Nizard R., Sedel L., Hannouche D., Hamadouche M. and Bizot P., Alumina pairing in total hip replacement, *J. Bone Joint Surg. Br.*, 2005; **87:** 755-758.

[4] Taskonak B., Yan J., Mecholsky J.J.J., Sertgöz A. and Koçak A., Fractographic analyses of zirconia-based fixed partial dentures, *Dent. Mater.*, 2008; **24:** 1077-1082.

[5] Masson B., Emergence of the alumina matrix composite in total hip arthroplasty, *Int. Orthop.*, 2009; **33:** 359-363.

[6] Hamadouche M. and Sedel L., Ceramics in orthopaedics, *J. Bone Joint Surg. Br.*, 2000; **82:** 1095-1099.

[7] Piconi C. and Maccauro G., Zirconia as a ceramic biomaterial, *Biomaterials*, 1999; **20:** 1-25.

[8] Phothawan A., Nganvongpanit K. and Tunkasiri T., Eitssayeam S. Study of mechanical properties of magnesium oxide doped alumina (Al 2O 3) and yttria stabilized zirconia (YSZ) composite for medical applications, *Adv. Mater. Res.*, 2012; **506:** 521-524

[9] Nganvongpanit K., Chaochird P., Siengdee P., Pothacharoen P., Klunklin K., Chomdej S., Mekchay S. and Kongtaweelert P., In vitro suppression of the MMP-3 gene in normal and cytokine-treated human chondrosarcoma using small interfering RNA, *J. Orthop. Surg. Res.*, 2009; 45.

[10] Nganvongpanit K., Müller H., Rings F., Gilles M., Jennen D., Hölker M., Tholen E., Schellander K. and Tesfaye D., Targeted suppression of E-cadherin gene expression in bovine preimplantation embryo by RNA interference technology using double-stranded RNA, *Mol. Reprod. Dev.*, 2006; **73:** 153-163.

[11] Nganvongpanit K., Müller H., Rings F., Hoelker M., Jennen D., Tholen E., Havlicek V., Besenfelder U. and Schellander K., Tesfaye D: Selective degradation of maternal and embryonic transcripts in in vitro produced bovine oocytes and embryos using sequence specific double-stranded RNA, Reproduction, 2006; **131:** 861-874.

[12] Thumdee P., Ponsuksili S., Murani E., Nganvongpanit K., Gehrig B., Tesfaye D., Gilles M., Hoelker M., Jennen D., Griese J., Hoelker M., Jennen D., Griese J., Schellander K. and Wimmers K., Expression of the prion protein gene (PRNP) and cellular prion protein (PrPc) in cattle and sheep fetuses and maternal tissues during pregnancy, *Gene Expr.* 2007; **13:** 283-297.

[13] Liagre B., Moalic S., Vergne P., Charissoux J.L., Bernache-Assollant D. and Beneytout J.L., Effects of alumina and zirconium dioxide particles on arachidonic acid metabolism and proinflammatory interleukin production in osteoarthritis and rheumatoid synovial cells, *J. Bone Joint Surg. Br.*, 2002; **84:** 920-930.

[14] Rimondini L., Cerroni L., Carrassi A. and Torricelli P., Bacterial colonization of zirconia ceramic surfaces: An in vitro and *in vivo* study, *Int. J. Oral Maxillofac. Implants*, 2002; **17:** 793-798.

[15] Scarano A., Piattelli M., Caputi S., Favero G.A. and Piattelli A., Bacterial adhesion on commercially pure titanium and zirconium oxide disks: An *in vivo* human study, *J. Periodontol.*, 2004; **75:** 292-296.

[16] Anderson J.M., Rodriguez A. and Chang D.T., Foreign body reaction to biomaterials, *Semin. Immunol.*, 2008; **20:** 86-100.

[17] Old L.J., Tumor necrosis factor, *Sci. Am.* 1988; **258:** 59-75.

[18] Amour A., Slocombe P.M., Webster A., Butler M., Knight C.G., Smith B.J., Stephens P.E., Shelley C., Hutton M., Knauper V., Docherty A.J. and Murphy G., TNF-alpha converting enzyme (TACE) is inhibited by TIMP-3, *FEBS Lett.*, 1998; **435:** 39-44.

[19] Barton B.E., IL-6: Insights into novel biological activities, *Clin. Immunol Immunopathol.*, 1997; **85:** 16-20.

[20] Di Santo E., Meazza C., Sironi M., Fruscella P., Mantovani A., Sipe J.D. and Ghezzi P., IL-13 inhibits TNF production but potentiates that of IL-6 *in vivo* and *ex vivo* in mice, *J. Immunol.*, 1997; **159:** 379-382.

[21] Xing Z., Gauldie J., Cox G., Baumann H., Jordana M., Lei X.F. and Achong M.K., IL-6 is an antiinflammatory cytokine required for controlling local or systemic acute inflammatory responses, *J. Clin. Invest.* 1998; **101:** 311-320.

[22] Ruzek M.C., Miller A.H., Opal S.M., Pearce B.D. and Biron C.A., Characterization of early cytokine responses and an interleukin (IL)-6-dependent pathway of endogenous glucocorticoid induction during murine cytomegalovirus infection, *J. Exp. Med.*, 1997; **185:** 1185-1192.

[23] Wimhurst J.A., Brooks R.A. and Rushton N., Inflammatory responses of human primary macrophages to particulate bone cements *in vitro*, *J. Bone Joint Surg. Br.* 2001; **83:** 278-282.

[24] Gupta S., Bi R. and Gollapudi S., Central memory and effector memory subsets of human CD4(+) and CD8(+) T cells display differential sensitivity to TNF-{alpha}-induced apoptosis, *Ann. N.Y. Acad. Sci.*, 2005; **1050:** 108-114.

[25] Boehm U., Klamp T., Groot M. and Howard J.C., Cellular responses to interferon-gamma, *Annu. Rev. Immunol.*, 1997; **15:** 749-795.

[26] Gessner A., Mohrs K. and Mohrs M., Mast cells, basophils, and eosinophils acquire constitutive IL-4 and IL-13 transcripts during lineage differentiation that are sufficient for rapid cytokine production, *J. Immunol.*, 2005; **174:** 1063-1072.

[27] McKenzie A.N., Li X., Largaespada D.A., Sato A., Kaneda A., Zurawski S.M., Doyle E.L., Milatovich A., Francke U. and Copeland N.G., Structural comparison and chromosomal localization of the human and mouse IL-13 genes, *J. Immunol.*, 1993; **150:** 5436-5444.

[28] Kasaian M.T. and Miller D.K., IL-13 as a therapeutic target for respiratory disease, *Biochem. Pharmacol.*, 2008; **76:** 147-155.

[29] de Waal Malefyt R., Figdor C.G., Huijbens R., Mohan-Peterson S., Bennett B., Culpepper J., Dang W., Zurawski G. and de Vries J.E., Effects of IL-13 on phenotype, cytokine production, and cytotoxic function of human monocytes. Comparison with IL-4 and modulation by IFN-gamma or IL-10, *J. Immunol.*, 1993; **151:** 6370-6381.

[30] Mijatovic T., Kruys V., Caput D., Defrance P. and Huez G., Interleukin-4 and -13 inhibit tumor necrosis factor-alpha mRNA translational activation in lipopolysaccharide-induced mouse macrophages, *J. Biol. Chem.*, 1997; **272:** 14394-14398.

[31] Jones J.A., McNally A.K., Chang D.T., Qin L.A., Meyerson H., Colton E., Kwon I.L., Matsuda T. and Anderson J.M., Matrix metalloproteinases and their inhibitors in the foreign body reaction on biomaterials, *J. Biomed. Mater. Res.* 2008; **84:** 158-166.

[32] Wan R., Mo Y., Zhang X., Chien S., Tollerud D.J. and Zhang Q., Matrix metalloproteinase-2 and -9 are induced differently by metal nanoparticles in human monocytes: The role of oxidative stress and protein tyrosine kinase activation, *Toxicol. Appl. Pharmacol.*, 2008; **233:** 276-285.